Design, Optimization and Control of a Cable-Driven Robotic Suit for Load Carriage

Yang Zhang and Vigen Arakelian

Abstract In recent years, exoskeletons show impressive results in the rehabilitation, field works, and military. However, their rigid structures lead to a lot of drawbacks like additional inertia and incompliant user interfaces. Comparing to the exoskeleton, exosuit is a wearable suit made by soft material and actuated by cable or pneumatic force, which is inherently compliant and much lighter. In this paper, an exosuit has been designed for assisting people while carrying heavy loads. For this exosuit, soft polyethylene braid-style cables are coupled with rigid frames that link with user's body through anchors and attachment points, which function as auxiliary muscles to apply force on both upper arm and forearm. The weight of the cables is negligible and adds nearly zero inertia to users. The proposed exosuit can function in two operation modes: passive and active modes. Static analysis and optimization are conducted for minimizing the cable tension and force exerted on user. Dynamic simulation shows that the proposed controller has good performance in active mode of the exosuit and experiments on the mannequin test bench validate its capability of holding loads with different postures in passive mode.

Keywords Exosuit · Wearable robotics · Upper limb · Dynamic modelling · Control

1 Introduction

The wearable robotic devices, also known as exoskeleton, have strong advantages given their unique features such as their outstanding physical performance, exceeding that of humans, and their mobility. As a result, attempts to adopt these devices in the rehabilitation and the industrial field provide a huge benefit for their users [1].

Y. Zhang · V. Arakelian (✉)
Team MECAPROCE, INSA-Rennes, Rennes, France
e-mail: vigen.arakelyan@insa-rennes.fr

LS2N UMR 6004, Nantes, France

Y. Zhang
Department SSE, HEI-Junia, Lille, France

V. Arakelian (ed.), *Gravity Compensation in Robotics*, Mechanisms and Machine Science 115, https://doi.org/10.1007/978-3-030-95750-6_5

Assistive robots have applications in the industrial field as well as for patients and the elderly with mobility impairments.

In the industrial field, work-related diseases of muscle and skeletal system are prevalent among physically demanding labors. Despite the industrialization has already been proceeding for hundreds of years, the number of occupational diseases, as well as cumulative trauma disorders (CTD) caused by overwork, is still significant nowadays. They are caused by ergonomic factors of the work environment, such as physical overload, compulsive working postures, the local stiffness of definite muscle groups and an adverse microclimate [2]. When workers carry loads, the gravity and dynamic force of the load will induce quite significant moments to the elbow, shoulder and trunk joint which will lead to the fatigue and even injury of muscles like the bicep, anterior deltoid, spinal extensor etc. [3].

Many researches in the field of wearable assistive robots have been conducted for augmenting the physical ability of human and minimizing work-related fatigue [4, 5]. The Berkeley Lower Extremity Exoskeleton (BLEEX) is powered by an internal combustion engine which is located in the backpack [12]. The hybrid engine delivers hydraulic power for locomotion and electrical power for the electronics. The exoskeleton is actuated via bidirectional linear hydraulic cylinders. BLEEX consumes an average of 1143 Watts of hydraulic power during level-ground walking, as well as 200 Watts of electrical power for the electronics and control. In contrast, a similarly sized, 75 kg human consumes approximately 165 W of metabolic power during level-ground walking. Instead of using powered components where actuator, control system, and power supply make the exoskeleton very bulky and heavy, some designs have been made with passive power sources like springs. By example, EXHAUSS offers a range of exoskeletons, each intended to relieve and protect operators, for various constraints related to handling or carrying loads or tools [6]. In these designs, springs are often used for gravity balancing of carrying loads. However, the support mechanical system is relatively heavy, and the handling is not easy. Additionally, the extra inertia effects must be compensated by users and the misalignment of the joints may cause the discomfort or even dangerous injuries.

For solving the previous problems, several soft, suit-like exoskeletons (also known as “exosuit”) have been proposed in recent years. Because of using soft materials like fabrics and cables, therefore, much less additional inertial effect is imposed to wearer’s movement. Additionally, since there is not any rigid joint in exosuits, so it has no joint misalignment problem. Several exosuits have been designed for upper-limb rehabilitation [7, 8] and power augmentation [9, 10]. In these exosuits, cables are anchored on user’s body by light-weight bracelets or flexible suit and winding actuators are used for tensioning cables and provide moment on the upper-limb joint. However, for the mentioned upper-limb exosuits, despite of the advantages of lightweight and compliant, they still some drawbacks like actuators are rather mounted on the user’s body but are mounted on the fixed frame or on the ground, which makes them unportable.

In order to reduce the moment generated by loads during transporting, in this paper, an exosuit for load carriage has been proposed. In this exosuit, polyethylene braid-style cables function as auxiliary muscles to augment the power of human. The exoskeleton has two function mode: passive and active. In passive mode, a locking mechanism will keep cables in tension and holding user's position during load carriage. And in active mode, actuators will provide suitable cable tension while user is carrying load and moving his arm.

The paper is organized as follows. At first, the design concept of the exosuit for carrying heavy load is presented. Then, the kinematic and dynamic model of exosuit-user coupled system is constructed in the third section. In the fourth section optimizations are made for reducing cable tensions and the workspace or exosuit is analyzed. Next, a controller is designed for the active mode of exosuit and simulations are carried out for evaluating its performance. Experiments on a mannequin test bench and results show in the sixth section. Conclusions are made in the last section.

2 Design Concept

In this study, a soft robotic suit to assist users for carrying heavy loads is proposed. This robotic suit is planned to have three features: 1) lightweight: the mass of the suit adds little extra inertia hence user's movement will not be impeded while wearing the robotic suit; 2) compliant: the interface between user and suit is compliant so user will not be hurt due to the installation error or system failure; 3) passive mode: the robotic suit can work in a passive mode where no actuation forces are need.

2.1 Development of the Robotic Suit's Rigid Frame

The rigid frame of the robotic suit consists of five parts: a main frame which fixed on the user's body, two upper arm bracelets which fixed with the user's upper arm, and two forearm bracelets which fixed with the user's forearm. The whole rigid frame is illustrated in Fig. 1.

In the main frame of the robotic suit, an adjustable plastic belt is at the bottom of the frame, and when users wear the suit, it fastens on the user's waist as a fixing component of the suit. Two shoulder pads are linked with the belt through two adjustable curved beams which can adapt to users with different height, and between these two beams, six horizontal beams are fixed between them to increase the whole structural strength. In order to create a comfortable interface between the shoulder pad, soft foam materials are stuck at the back of the shoulder pads.

Fig. 1 Rigid frame of the robotic suit

All the four bracelets have a similar structure which consist of two rings a curve pad linked with the rings. The rings are adjustable which can adapt the size of the user's arms. The pads can avoid force concentration since they increase the contact surface between the bracelet and the user's arm. Similar to the should pad, soft foam materials are also used at the interface between the bracelet and the user's arm for enhancing comfortability.

It should be also noticed that on all the bracelets and shoulder pads, there are some pins combined with some small rings on them, and these are the cable anchors and cable attachment points. We define an anchor is where the cable starts from, the cable is fixed with the small ring. And an attachment point is where the cable only passes through the small ring. For the shoulder pads and upper arm bracelets, the pins are fixed on them, and for the forearm bracelets, the pins are inserted into the groove on the rings which allow the pins have a translational movement along the rings. Thus, the pronation/supination movement of the forearm will not change the position of the anchors and attachment points on the forearm bracelets. The positions of attachment points and anchors are optimized in the previous research for minimizing the cable tension [11].

2.2 Coupling of Cables with the Rigid Frame

When humans want to move their arms, their muscles contract for generating tension forces; then the forces are transmitted to the skeletons through tendons hence moments will be generated on the articulations for moving their limbs.

In the proposed robotic suit, the cables are used for similar functionality as the human muscles where the cable tension is the muscle's contract force. The cables can transmit forces on the user's arm through arm bracelets and with accurate control

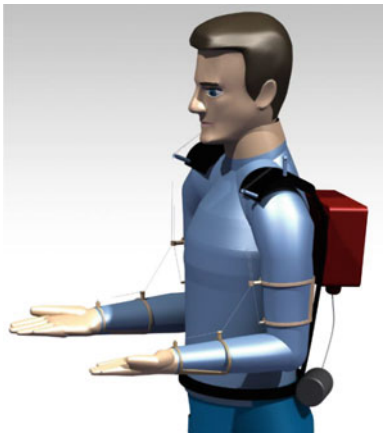

Fig. 2 3D model of the robotic suit

of the tensions of the cables, a desirable assistive performance can be obtained by users during load carriage.

The cables for the robotic suit are the polyethylene braid-style cables fabricated by Caperlan which is originally used for fishing. The diameter of the cable is only 0.4 mm and the weight is extremely light. The cable can hold up a load up to 34 kg, while in the meantime only have a tiny deformation.

Figure 2 illustrates a 3D model where a user wears the proposed robotic suit where cables are coupled with the rigid frame and the batteries, control system and motors are mounted on the rigid frame. For each of the user's arm, two cables are started from the anchors on forearm and upper arm, respectively; then pass through the attachment points on the arm and shoulder and then through the inside of the hollow beam which links the shoulder pad and the belt; finally end at spool on the motor which is mounted on the belt.

2.3 Robotic Suit Operation

When humans want to move a load from one place to another place, normally the transportation can be separated into three phases. The first phase is to let the hands approach the load, then grab it and hold it with a comfortable posture. Then the phase is to hold the load and walk to the final destination where we want to put the load. The last phase is a discharge prosses in which we adjust our arms to adapt to the place where we want to put the load at, for example, a shelf.

(a) **Passive mode**

It can be seen that during the second phase of the load transportation, one stays at a quasi-fixed posture, and the moments generated on the arm's joints are mainly due to gravity and stay relatively constant. Therefore, in this phase, we can let the all the

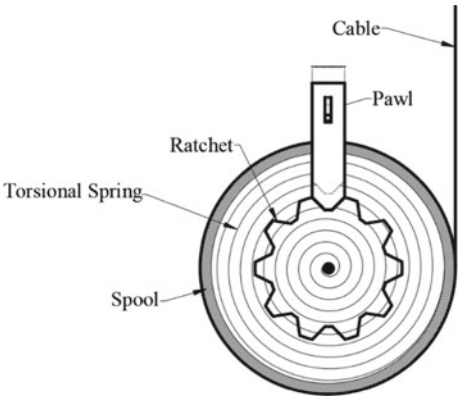

Fig. 3 Cable locking mechanism

cables in tension and stop the movement of the cables, then the movement of user's arm will be constrained, and the moment induced by the gravity will be transmitted on the shoulder. Thus, the fatigue of the muscle on the arms due to holding load will be relived.

Instead of letting the motors generating torque to hold the position of the cable which needs a lot of energy if the distance from the start point and destination is too far, a cable winding and locking mechanism (shown in Fig. 3) was designed. This mechanism includes a cable spool, a torsional spring, and a ratchet mechanism. The cable spool links with the torsional spring and the ratchet. The torsional spring can provide a suitable passive moment for the spool to keep the cable always in tension while users moving their arms. And the ratchet mechanism is used as a locking mechanism to stop the movement of the cable. When wearers pick up the load and hold it in a comfortable position, the locking mechanism can be engaged by pressing the controller on their hands. Then the pawl moves down and enters the gap between two teeth of the ratchet. Consequently, the spool is stopped from moving and the passively generated cable tension can be used for compensating the gravity of the load. In contrast, when the user is not carrying loads, the pawl will lift and the spool can freely rotate.

(b) **Active mode**

Unlike the second phase of the load carriage where user's arms stay at a fixed posture and only constant forces are needed for compensating the gravitational effect, in the first and the third phase of the load carriage, wearers need to hold the load and move it to the expected position. Therefore, in these phases, variable forces will be required since the dynamic effect will occur, and the forces utilized to compensate the gravitational effect will vary as the user changing their arms postures.

In the proposed design, four DC motors are linked the cable spools providing active forces to the four cables, respectively. The torques of the motors are controlled through an on-board closed-loop controller. The pose data obtained by the potentiometers mounted on the joints of the arm can be used by the on-board controller.

For the safety of the users, when robotic suit works in active mode, the maximum force provided to the cable is limited to 150 N for all the cables. Additionally, there is also a safety button for cutting off the power source if any emergency happens.

3 Modelling of the Coupled System

3.1 Kinematic Modelling

The user carrying the load while wearing the robotic suit can be in analogy with a coupled system including a 2-DOF planar mechanical structure with the load at the end effector and cables attached on the manipulator for exerting forces.

A planar diagram of a user wearing the exosuit system is shown in Fig. 4. In this diagram, two cables start from the anchors on the forearm and upper arm respectively and end at the cable winding and locking mechanisms fixed on the hip. The cable arrangements are as following: cable 1 starts form anchor on point 1, pass through attachment points on point 2, point 4, point 5, point 6, point 7, point 8; cable 2 starts form anchor on point 3, pass through attachment points on point 4, point 5, point 6, point 7, point 8. It is assumed that the deformation of the cable is very tiny and negligible.

As shown in Fig. 4, two local coordinate systems $X_1O_1Y_1$ and $X_2O_2Y_2$ are fixed on the upper arm and forearm, respectively. The general coordinate of point i on the global coordinate system can be calculated by:

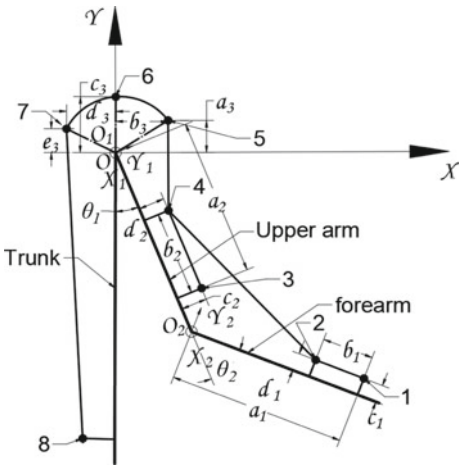

Fig. 4 Planar diagram of the distribution of anchors and attachment points while user wearing the robotic suit

$$\mathbf{p}_i = \begin{bmatrix} x_i \\ y_i \\ 1 \end{bmatrix} = \begin{cases} {}^{0}_{1}\mathbf{Trans} \cdot \mathbf{p}_i^1 \\ {}^{0}_{1}\mathbf{Trans} \cdot {}^{1}_{2}\mathbf{Trans} \cdot \mathbf{p}_i^1 \end{cases} \tag{1}$$

where,

$${}^{0}_{1}\mathbf{Trans} = \begin{bmatrix} \cos(3\pi/2+\theta_1) & -\sin(3\pi/2+\theta_1) & 0 \\ \sin(3\pi/2+\theta_1) & \cos(3\pi/2+\theta_1) & 0 \\ 0 & 0 & 1 \end{bmatrix}$$

$${}^{1}_{2}\mathbf{Trans} = \begin{bmatrix} \cos\theta_2 & -\sin\theta_2 & l_{ar} \\ \sin\theta_2 & \cos\theta_2 & 0 \\ 0 & 0 & 1 \end{bmatrix}$$

and $\mathbf{p_i^1}$ and $\mathbf{p_i^2}$ stand for the local general coordinates of point i in local coordinate systems $X_1O_1Y_1$ and $X_2O_2Y_2$ respectively, l_{tr} is the length of the trunk and l_{ar} is the length of the upper arm.

Thus, the global coordinate of point i is:

$$\boldsymbol{c}_i = \begin{bmatrix} x_i \\ y_i \end{bmatrix} \tag{2}$$

For both two cables, they all have a fixed length through attachment points 5, 6, 7, and 8 since all these points are fixed on the user's trunk. Let us define this fixed length as l_0. And as shown in Fig. 4, the local general coordinates of point 1, 2, 3, and 4 are $\mathbf{p_1^1} = [a_1, c_1, 1]$, $\mathbf{p_2^1} = [a_1{-}b_1, d_1, 1]$, $\mathbf{p_3^2} = [a_2, c_2, 1]$, $\mathbf{p_4^2} = [a_2{-}b_2, d_2, 1]$, and the global coordinate of point 5 is $\mathbf{c_5} = [b_3, a_3]$. Then the lengths of cable 1 and cable 2 can be calculated by:

$$\begin{cases} l_1 = f_1(\theta_1, \theta_2) \\ l_2 = f_2(\theta_1) \end{cases} \tag{3}$$

Then, using the time derivative of Eq. (3), the relationship between the cable velocity and the angular velocity of the user's joints can be obtained by:

$$\begin{bmatrix} \dot{l}_1 \\ \dot{l}_2 \end{bmatrix} = \mathbf{J_v} \begin{bmatrix} \dot{\theta}_1 \\ \dot{\theta}_2 \end{bmatrix} \tag{4}$$

where $\dot{l}_1$ and $\dot{l}_2$ denote the cable velocities.

The detailed information of function $f_1(\theta_1,\theta_2)$, $f_2(\theta_1)$ and matrix $\mathbf{J_v}$ can be found in Appendix.

3.2 Dynamic Modelling

The general dynamic equations of the coupled system can be obtained from the Lagrangian formulation where the generalized coordinate is $\boldsymbol{q} = [\theta_1, \theta_2]^T$. Lagrange's equation can be written in the form of kinetic energy K, potential energy V and generalized forces or torques $\mathbf{Q}$ in the following form:

$$\frac{d}{dt}\left(\frac{\partial K(\boldsymbol{q}, \dot{\boldsymbol{q}})}{\partial \dot{\boldsymbol{q}}}\right) - \frac{\partial K(\boldsymbol{q}, \dot{\boldsymbol{q}})}{\partial \boldsymbol{q}} + \frac{\partial V(\boldsymbol{q})}{\partial \boldsymbol{q}} = \boldsymbol{Q} \tag{5}$$

The kinetic energy of the coupled system combines three parts: kinetic energy of the upper arm K_1, kinetic energy of the forearm K_2, and kinetic energy of the load K_3. They can be calculated by:

$$K_1 = \frac{1}{2} I_{ua} \dot{\theta}_1^2 + \frac{1}{2} m_{ua} l_{cua}^2 \dot{\theta}_1^2 \tag{6}$$

$$K_2 = \frac{1}{2} I_{fa} \left(\dot{\theta}_1 + \dot{\theta}_2\right)^2 + \frac{1}{2} m_{fa} \left[l_{ua}^2 \dot{\theta}_1^2 + l_{cfa}^2 \left(\dot{\theta}_1 + \dot{\theta}_2\right)^2 + 2 l_{ua} l_{cfa} cos\theta_2 \left(\dot{\theta}_1^2 + \dot{\theta}_1 \dot{\theta}_2\right) \right] \tag{7}$$

$$K_3 = \frac{1}{2} m_{load} \left[l_{ua}^2 \dot{\theta}_1^2 + l_{cload}^2 \left(\dot{\theta}_1 + \dot{\theta}_2\right)^2 + 2 l_{ua} l_{cload} cos\theta_2 \left(\dot{\theta}_1^2 + \dot{\theta}_1 \dot{\theta}_2\right) \right] \tag{8}$$

where I_{ua} and I_{fa} are the moment of inertias of upper arm and forearm respectively; m_{ua}, m_{fa} and m_{load} are the masses of upper arm, forearm, and load respectively; l_{ua} is the lengths of upper arm; l_{cua} is the distances between the center of mass of upper arm to the shoulder joint, l_{cfa} and l_{cload} are the distances between the centers of mass of forearm and load to the elbow joint.

In this study, the elastic and damping effects of cable are neglected, and each cable is assumed to be a force element. Therefore, the potential energy of the system is only due to the gravitational effect and the total potential energy is:

$$\begin{aligned} V = & -m_{ua} g l_{cua} (\cos\theta_1 - 1) + m_{fa} g \left[l_{ua} (1 - \cos\theta_1) + l_{cfa} (1 - \cos(\theta_1 + \theta_2)) \right] \\ & + m_{load} g [l_{ua} (1 - \cos\theta_1) + l_{cload} (1 - \cos(\theta_1 + \theta_2))] \end{aligned} \tag{9}$$

where g is the gravity acceleration.

In the coupled system, the generalized torques are induced by the cable tension trough anchors and attachment points on the user's arm. It is obvious that the torques have a relationship with the geometrical distribution of the anchors and attachment points. The moments on the elbow and shoulder joint generated by cable 1 and 2 can be calculated by:

$$\begin{aligned} M_{shoulder}^{cable1} &= \left[\boldsymbol{v}_{O_11}^* \times \boldsymbol{v}_{12} + \boldsymbol{v}_{O_12}^* \times (\boldsymbol{v}_{21} + \boldsymbol{v}_{24}) + \boldsymbol{v}_{O_14}^* \times (\boldsymbol{v}_{42} + \boldsymbol{v}_{45})\right] \cdot T_1 \\ M_{elbow}^{cable1} &= [\boldsymbol{v}_{O_21}^* \times \boldsymbol{v}_{12} + \boldsymbol{v}_{O_22}^* \times (\boldsymbol{v}_{21} + \boldsymbol{v}_{24})] \cdot T_1 \\ M_{shoulder}^{cable2} &= [\boldsymbol{v}_{O_23}^* \times \boldsymbol{v}_{34} + \boldsymbol{v}_{O_24}^* \times (\boldsymbol{v}_{43} + \boldsymbol{v}_{45})] \cdot T_2 \\ M_{elbow}^{cable2} &= 0 \end{aligned} \tag{10}$$

where,

$$\boldsymbol{v}_{ij}^* = \boldsymbol{c}_j - \boldsymbol{c}_i$$

$$\boldsymbol{v}_{ij} = \frac{\boldsymbol{c}_j - \boldsymbol{c}_i}{\left|\boldsymbol{c}_j - \boldsymbol{c}_i\right|}$$

$\boldsymbol{c_i}$ is the global coordinate of point i.

The total moments on shoulder and elbow joints induced by the cable tensions can be calculated by:

$$\begin{bmatrix} M_{shoulder}^{cable} \\ M_{elbow}^{cable} \end{bmatrix} = \begin{bmatrix} M_{shoulder}^{cable1} + M_{shoulder}^{cable2} \\ M_{elbow}^{cable1} + M_{elbow}^{cable2} \end{bmatrix} = \boldsymbol{J_M} \begin{bmatrix} T_1 \\ T_2 \end{bmatrix} \tag{11}$$

where,

$$\boldsymbol{J_M} = \begin{bmatrix} \boldsymbol{v}_{O_21}^* \times \boldsymbol{v}_{12} + \boldsymbol{v}_{O_22}^* \times (\boldsymbol{v}_{21} + \boldsymbol{v}_{24}) + \boldsymbol{v}_{O_24}^* \times (\boldsymbol{v}_{42} + \boldsymbol{v}_{45}) & \boldsymbol{v}_{O_23}^* \times \boldsymbol{v}_{34} + \boldsymbol{v}_{O_24}^* \times (\boldsymbol{v}_{43} + \boldsymbol{v}_{45}) \\ \boldsymbol{v}_{O_31}^* \times \boldsymbol{v}_{12} + \boldsymbol{v}_{O_32}^* \times (\boldsymbol{v}_{21} + \boldsymbol{v}_{24}) & 0 \end{bmatrix}$$

Through substituting Eq. (6)–(9) into Eq. (5), the general dynamic equation of the coupled system in terms of generalized coordinates can be obtained as the following form:

$$\boldsymbol{M}(\boldsymbol{q})\ddot{\boldsymbol{q}} + \boldsymbol{C}(\boldsymbol{q}, \dot{\boldsymbol{q}})\dot{\boldsymbol{q}} + \boldsymbol{G}(\boldsymbol{q}) = \boldsymbol{J_M}\begin{bmatrix} T_1 & T_2 \end{bmatrix}^T \tag{12}$$

where $\mathbf{M}(\mathbf{q})$ is the inertia matrix of the system, $\boldsymbol{C}(\boldsymbol{q}, \dot{\boldsymbol{q}})$ is the matrix of Coriolis and centripetal terms, $\mathbf{G}(\mathbf{q})$ is the vector of gravity terms. The detailed form of Eq. (12) can be found in Appendix.

4 Optimization and Work Space Analysis

4.1 Static Simulations and Optimization

When people carry an object at a relatively fixed position, their arms undertake the load generally due to the gravitational effect of the arm. The gravity of object and arm generate moments on the shoulder and elbow joints which must be compensated by our muscle force. The moment on the shoulder and elbow joints induced by the gravitational force is $\mathbf{G}(\mathbf{q})$ term in Eq. (12) and it can be calculated by:

$$\begin{aligned} M_{shoulder}^{gravity} &= m_{ua} g l_{cua} \sin\theta_1 + m_{fa} g\left[l_{ua} \sin\theta_1 + l_{cfa} \sin(\theta_1 + \theta_2)\right] + m_{load} g\left[l_{ua} \sin\theta_1 + l_{cload} \sin(\theta_1 + \theta_2)\right] \\ M_{elbow}^{gravity} &= \left(m_{fa} l_{cfa} + m_{load} l_{cload}\right) g \sin(\theta_1 + \theta_2) \end{aligned} \tag{13}$$

The average body segment parameters of an adult male with 172.68 cm height and 63.97 kg weight are given in Table 1 [13]. Using these parameters, the gravity moments on waist, shoulder, and elbow joint when carrying a 10 kg load with different postures ($\theta_1 \in [0°, 45°]$, $\theta_2 \in [0°, 90°]$) are shown in Fig. 5. It is shown that when carrying the load with different postures, the gravitational moments on the joints also vary and these moments must be compensated by the muscle force.

Table 1 Body segment parameters of an adult male

	Mass (kg)	Length (m)	Location of COM (m)
Upper arm	2.07	0.364	0.182
Forearm	1.7	0.299	0.149

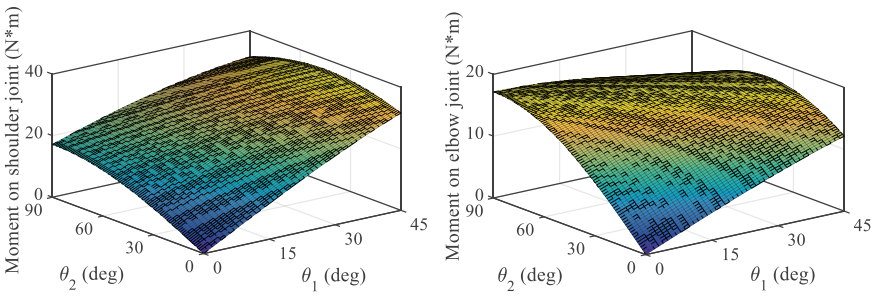

(a) Gravitational moment on shoulder joint (b) Gravitational moment on elbow joint

Fig. 5 Gravitational moment on the shoulder (a) and elbow (b) joint when carrying a 10 kg load with different postures

When a user wears the exosuit which is in passive mode, the cable locking mechanism is engaged, and the gravitational effect of the load and arm can be compensated by cables and distributed on the shoulder. According to Eq. (11), the cable tensions for compensating the gravitational effect can be solved by:

$$\begin{bmatrix} T_1^{gravity} \\ T_2^{gravity} \end{bmatrix} = \mathbf{J}_\mathbf{M}^{-1} \begin{bmatrix} M_{shoulder}^{gravity} \\ M_{elbow}^{gravity} \end{bmatrix} \tag{14}$$

and the force applied on the shoulder by cables is:

$$\mathbf{F}_{shoulder}^{gravity} = \mathbf{v}_{54}(T_1^{gravity} + T_2^{gravity}) \tag{15}$$

The elements in the matrix $\mathbf{J_M}$ are determined by the geometrical distribution of anchors and attachment points. To investigate the cable tensions during the usage of the exosuit in passive mode, at first, we chose the initial positions of anchor and attachment points as following: $a_1 = 0.3$ m, $b_1 = 0.1$ m, $c_1 = 0.08$ m, $d_1 = 0.08$ m, $a_2 = 0.26$ m, $b_2 = 0.1$ m, $c_2 = 0.1$ m, $d_2 = 0.1$ m, $a_3 = 0.65$ m, $b_3 = 0.1$ m, $c_3 = 0.1$ m, $d_3 = 0.1$ m *and* $e_3 = 0.1$ m.

Figure 6 shows the cable tensions when the user carries a 10 kg load with different arm postures, where the maximum tensions are 130 N and 711 N for cable 1 and 2, respectively. It should be noticed that, for the maximum tension in cable 2, the limit of the max tolerable tension has already been passed. Besides, for some postures, the tension of cable 2 is negative which is not permissible.

Another thing must be concerned with is the force exerted on the shoulder by cables, since a large portion of force has been redistributed on the shoulder. Figure 7 shows the force on the shoulder while the user carrying a 10 kg load with different postures. It can be seen the maximum force on the shoulder reaches up to 1355 N, and this amount of force will be harmful for users.

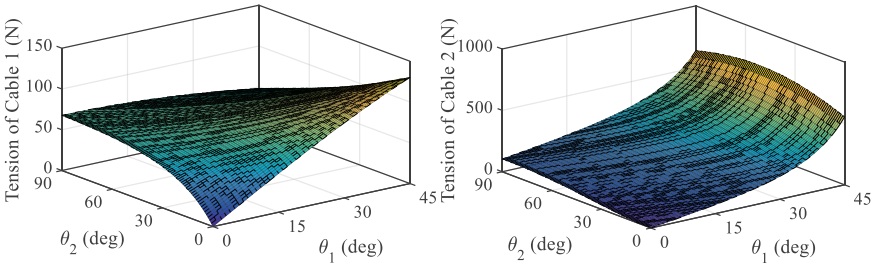

(a) Tension of Cable 1 (b) Tension of Cable 2

Fig. 6 Cable tensions when carrying a 10 kg load with different postures

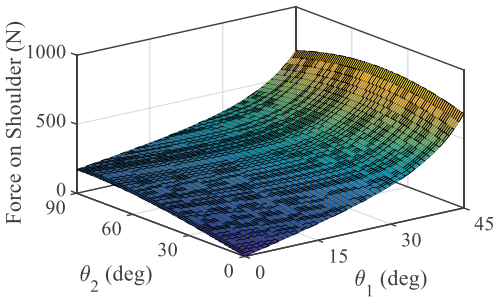

Fig. 7 Force on the user's shoulder when carrying a 10 kg load with different postures

It is obvious that the initial locations of the anchors and attachment points are not suitable for our robotic suit since the large cable tension and the large pressure on the shoulder. Therefore, in order to have a suitable arrangement of anchors and attachment points, their locations must be optimized.

In the optimization, we take Matlab *fmincon* function as our optimization algorithm and the parameters which are going to be optimized are $a_1, b_1, c_1, d_1, a_2, b_2, c_2, d_2, a_3, b_3, c_3, d_3, and\ e_3$ (as shown in Fig. 4). For the possible postures of the user, we choose the arm configurations as $\theta_1 \in [0°, 15°, ..., 45°]$ and $\theta_2 \in [0°, 10°, ..., 90°]$ which gives us 40 possible postures. In this optimization, we are going to minimize the total cable tensions and force exerted on the shoulder when the user carrying a 10 kg load with these 40 possible postures.

Another thing has to be concerned is the constraints. In our problem, there is two kinds of constraints which are:

(1) For all the configurations, cables must be always in tension i.e., cable tensions are always positive.
(2) The space constraints of the positions of anchors and attachment points.

Hence the problem in this optimization can be concluded as:

$$\min_{a_1,b_1,...,e_3} \left[\sum_{\theta_1} \sum_{\theta_2} \left(T_1^{gravity} + T_2^{gravity} + T_{shoulder}^{gravity} \right) + P \right] \tag{16}$$

$$\begin{aligned} \text{subject to : } & 0.2 \le a_1 \le 0.3;\ 0.01 \le b_1 \le 0.1;\ 0.08 \le c_1 \le 0.13; \\ & 0.08 \le d_1 \le 0.13;\ 0.16 \le a_2 \le 0.26;\ 0.01 \le b_2 \le 0.1; \\ & 0.1 \le c_2 \le 0.15;\ 0.1 \le d_2 \le 0.15;\ 0.55 \le a_3 \le 0.7; \\ & -0.1 \le b_3 \le 0.1;\ 0.05 \le c_3 \le 0.15;\ -0.1 \le d_3 \le 0.1; \\ & 0.05 \le e_3 \le 0.15. \end{aligned}$$

where P is a very large value to penalize the goal function when any of the cable tension is negative for all configurations.

After applying fmincon function in Matlab, the obtained optimal parameters are the followings: $a_1 = 0.23$ m, $b_1 = 0.1$ m, $c_1 = 0.11$ m, $d_1 = 0.08$ m, $a_2 = 0.26$ m, $b_2 = 0.01$ m, $c_2 = 0.14$ m, $d_2 = 0.15$ m, $a_3 = 0.7$ m, $b_3 = -0.1$ m, $c_3 = 0.15$ m, $d_3 = 0$ m *and* $e_3 = 0.05$ m. With these parameters, the cable tensions with respect to

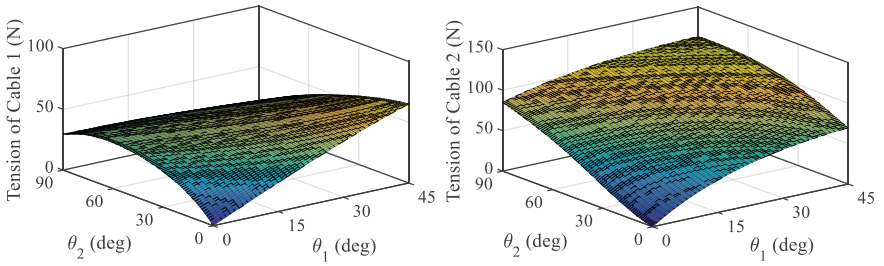

(a) Tension of Cable 1 (b) Tension of Cable 2

Fig. 8 Cable tensions when carrying a 10 kg load with different postures after optimization

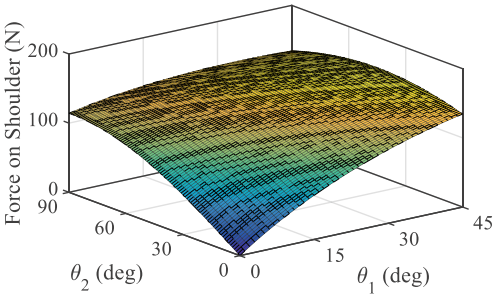

Fig. 9 Force on the user's shoulder when carrying a 10 kg load with different postures after optimization

different postures are shown in Fig. 8. It can be seen that after optimization the cable tensions have been drastically reduced, with maximum values of 65 N and 114 N for cable 1 and cable 2 respectively. Meanwhile, as shown in Fig. 9, the force exerted on the shoulder has also been generally diminished, with the maximum value of 304 N. Therefore, after optimization, the exosuit is more suitable and comfortable to wear.

4.2 Workspace Analysis

Unlike the traditional exoskeleton in which the actuation forces are transmitted through rigid links to the user, in the proposed robotic suit, cables are used as the transmission media. Therefore, limited by the characteristic of the cable, only tension forces can be transmitted.

While the determination of the workspace of the exosuit, the physical limitation of the cable must be considered. Hence, we can define the workspace of the exosuit as a set of joint angles [$\theta i\ 1$, $\theta i\ 2$] which fulfill the following condition:

$$T_k^{gravity}\left(\theta_1^i, \theta_2^i\right) \geq 0\,(k = 1 \text{ and } 2) \tag{17}$$

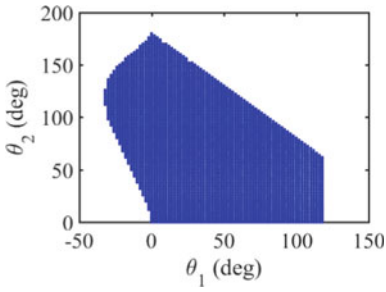

Fig. 10 Workspace of the propose exosuit

For investigating the workspace of the proposed robotic suit, the arm configurations which satisfy the condition described in Eq. (17) were found taking the optimal positions of the anchors and attachment point which was obtained in the previous part.

Figure 10 shows all the possible arm configuration of the exosuit. The workspace comprises most part of the real configurations of the human arm except for some part when the upper arm is in extension (the humerus is rotated out of the plane of the torso so that it points backward) or upper arm has large flexion angle.

5 Controller Design and Dynamic Simulation

When users want to pick up the load on the ground or put the load on a high shelf, their posture must be changed to adjust the vertical level of the load. Therefore, unlike the robotic suit works in passive mode, a controller must be needed for providing the different actuating force with respect to different postures. In addition, the dynamic effect of the user's arm and load must be taken into consideration.

In the proposed design, a closed loop control based on a PD controller and a feedforward term for gravity compensation is utilized for controlling the active force. Potentiometers are mounted on the user's arms for the measurement of elbow and shoulder joint angles. It should be noticed that, for the controlled output forces, only positive values can be provided since only tension forces can exist in the cables. The final controlled active force can be expressed as the following:

$$\mathbf{T_{active}} = max\left\{\mathbf{J_M^{-1}}(\boldsymbol{\theta})\left[\mathbf{K_p}(\boldsymbol{\theta_d} - \boldsymbol{\theta}) + \mathbf{K_d}\left(\dot{\boldsymbol{\theta}}_\mathbf{d} - \dot{\boldsymbol{\theta}}\right) + \mathbf{G}(\boldsymbol{\theta_d})\right], \left[0\ 0\right]^T\right\} \tag{18}$$

where $\boldsymbol{\theta}_d$ and $\dot{\boldsymbol{\theta}}_d$ are the desired joint angles and joint velocities; $\mathbf{K_p}$ and $\mathbf{K_d}$ are the diagonal matrices consist of proportional and derivative gains of the PD controller respectively.

A block diagram of the proposed controller is shown in Fig. 11. It can be seen that a prescribed desired state of the system is given as the input. A feedforward loop which is comprised of the gravity compensation to eliminate the effect of gravitational force.

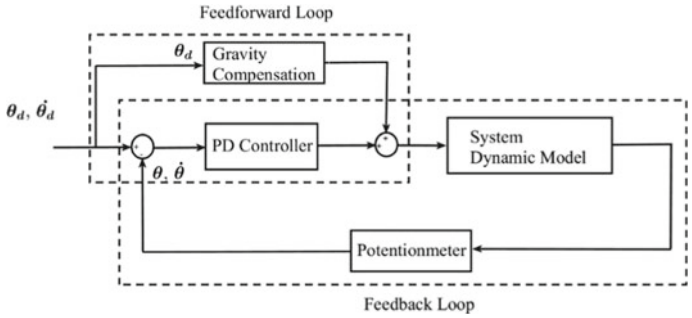

Fig. 11 Block diagram of the PD controller with gravity compensation

A feedback loop consists of a PD controller which uses the measured real state of the system to generate appropriate dynamic forces which actuate the system to the desired state.

Additionally, in order to let simulation model be more realistic to the working environment, an extra term has been added on the system dynamic model representing nonlinear external disturbances (e.g., vibration during walking, etc.). These disturbances are modeled as random white noises in the proposed model.

For generating a smooth trajectory between the initial position and final desired position, a trajectory generation method based on sinusoidal function has been utilized. The trajectory of a joint can be represented by the following equations:

$$q(t) = \begin{cases} q_i + \frac{q_f - q_i}{2}\left[sin\left(\frac{t}{\tau}\pi - \frac{\pi}{2}\right) + 1\right] (t \leq \tau) \\ q_f \ (\mathrm{t} > \tau) \end{cases} \tag{19}$$

where q_i is the initial position, q_f is the final desired position and τ is the duration of the sinusoidal trajectory.

Based on the dynamic model described in the previous section, a Simulink model of the proposed system has been built. Dynamic simulations of the system have been carried out via the Simulink model for validating the effectiveness of the controller and the exosuit's operation in active mode. And for demonstrating the system having the capability of coping with various trajectories, four different trajectories have been chosen based on previously proposed trajectory generation method. The parameters of these trajectories are shown in Table 2.

Table 2 Parameters of the trajectories

	q_{i1} (deg)	q_{f1} (deg)	τ_1 (s)	q_{i2} (deg)	q_{f2} (deg)	τ_2 (s)
1	0	0	0	0	90	5
2	0	20	1.11	0	70	3.89
3	45	0	2.5	45	90	2.5
4	90	0	5	0	90	5

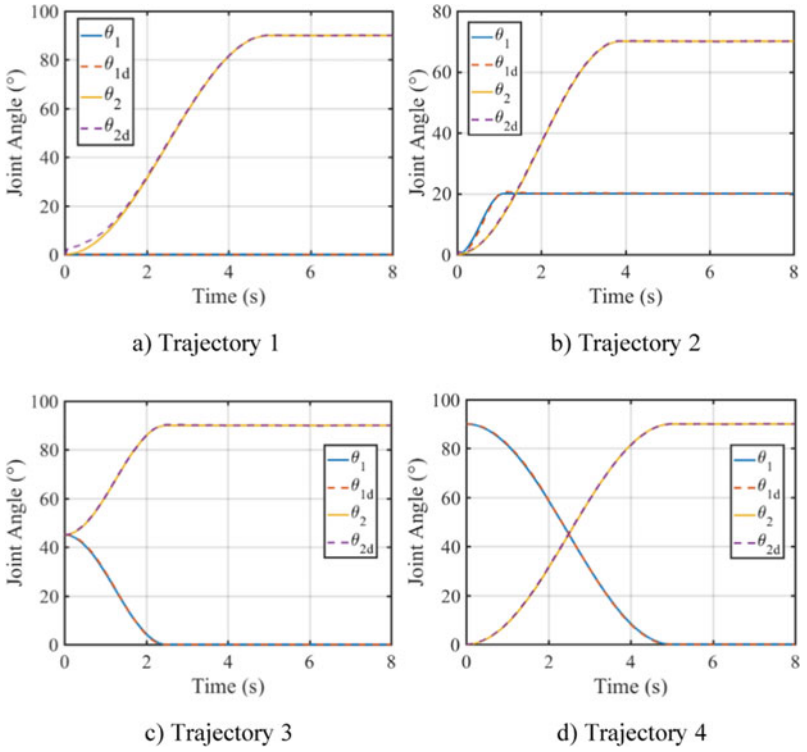

Fig. 12 Comparison of the actual and desired trajectories

In Fig. 12, the solid lines show the variations of joint angles during simulation and the dash lines shows the desired input trajectories to follow. It can be noticed that, for all four trajectories, the robotic suit shows high tracking performance with the help of the proposed PD controller. The robot suit follows the prescribed trajectories quite accurately even under the external random disturbances.

The cable tensions (which is also the active force in robotic suit system) during the different trajectory tracking are shown in Fig. 13. It can be seen that the cable tension fluctuates during the simulations, which is a response to the external disturbance controlled by PD controller. In most of the situations, the cable tension is under 120 N which is a quite safe value since the cable can hold the tension up to 340 N.

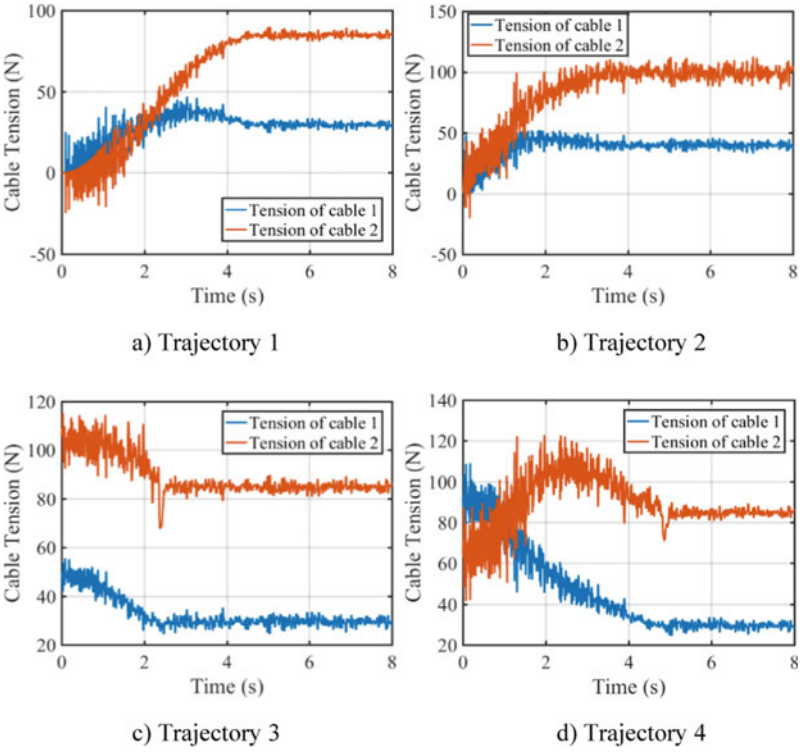

Fig. 13 Cable tensions for the tested trajectories

6 Experimental Validation

To evaluate the performance of proposed passive exosuit, a testbench was fabricated as shown in Fig. 14. The test bench was converted from a mannequin where spherical joints were added on the elbow joints and shoulder joints.

To test the performance of the exosuit when a user is in different postures, several postures have been chosen in this experiment. For the shoulder extension angle, we chose 0° and 30°, and for the forearm flexion angle 0°, 30°, 60°, and 90° were chosen. And for each posture, we put no load, 5 kg load, and 10 kg load respectively. Then the cable tensions were measured.

When the experiments were conducted with different postures and different load, with the help of the exosuit, the mannequin test bench can hold the load steadily in the designated postures. The change of the cable tensions with respect to the change of forearm flexion angle when shoulder extension angle is 0° and 30° are shown in Fig. 15 and Fig. 16 respectively.

Fig. 14 Mannequin test bench **(a)** and the added joints **(b, c)**

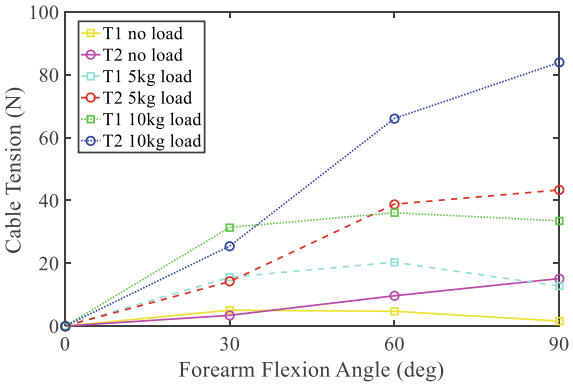

Fig. 15 Cable tensions with respect to the change of forearm flexion angle (shoulder extension angle is 0°)

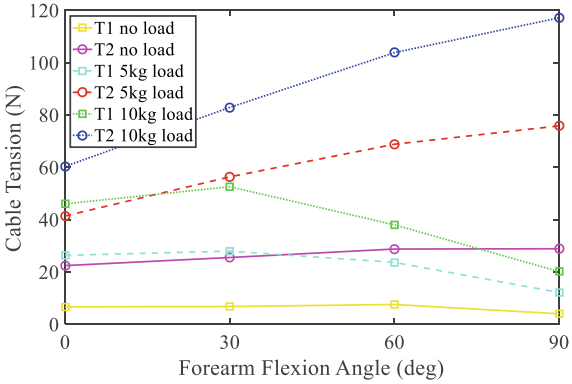

Fig. 16 Cable tensions with respect to the change of forearm flexion angle (shoulder extension angle is 30°)

7 Conclusion

A robotic suit has been proposed which intends to assist its user in the carriage of heavy load in this paper. The proposed robotic suit presents a symbiosis of two systems: a rigid support frame and a cable system. The cable system is coupled with the rigid support frame providing assistive force to its users during load carriage and it is made up of high-intensity polyethylene cables, which are very light and add almost zero inertia to users. A cable locking mechanism has been designed in order to keep cables in tension and to stop the movement of the cables.

The robotic suit has two operation modes: passive and active modes. When wearers hold the load at a fixed posture, the cable locking mechanism is engaged to stop the movement of the cable and the robotic suit works in the passive mode where no energy is needed. When users change their postures while holding the load, the robotic suit works in the active mode providing variable assistive forces with respect to the movement.

The kinematic and dynamic models of the robotic suit system have been built. Static simulation has been carried out via the built model and an optimization of the position of the anchors and attachment points of the robotic suit has been made by using fmincon function in Matlab for minimizing the cable tension and force exerted on the shoulder. The workspace of the robotic suit has been analyzed for showing the possible posture while wearing the exsosuit.

Dynamic model of the exosuit-human coupled system has been built. A PD controller with gravitational force compensator was designed. Dynamic simulations of the robotic suit in trajectory tracking have been carried out via Matlab Simulink. All the simulations showed that the proposed controller had good performances during working in active mode and the maximum cable tension is around 120 N which is much lower than the maximum supportable tension.

In order to evaluate the performance of the robotic suit in a more realistic environment and validate the simulation results, a mannequin test bench has been fabricated

and tested. The test results showed that with the help of the robotic suit, the mannequin can hold different weights of loads steadily in different postures.

In the future study, a prototype of the proposed exosuit with actuators integrated into a jacket plans to be developed. Then tests in the actual working scenario with exosuit in active mode will be conducted.

Appendix

This appendix shows the detailed form of the kinematic and dynamic equation of the coupled system Sect. 3.

The detailed form of the Eq. (3) is:

$$f_1(\theta_1,\theta_2) = \sqrt{\begin{matrix}[d_1\cos(\theta_1+\theta_2)+(a_1-b_1)\sin(\theta_1+\theta_2)-d_2\cos\theta_1-(a_2-b_2-l_{ar})\sin\theta_1]^2+\\ [(a_1-b_1)\cos(\theta_1+\theta_2)-d_1\sin(\theta_1+\theta_2)-(a_2-b_2-l_{ar})\cos\theta_1+d_2\sin\theta_1]^2\end{matrix}} + \sqrt{(a_3+a_2\cos\theta_1-b_2\cos\theta_1-d_2\sin\theta_1)^2+(b_3-d_2\cos\theta_1-a_2\sin\theta_1+b_2\sin\theta_1)^2}+\sqrt{b_1^2+(c_1-d_1)^2}+l_0 \tag{20}$$

$$f_2(\theta_1) = \sqrt{[a_3+(a_2-b_2)cos\theta_1-d_2sin\theta_1]^2+[b_3-d_2cos\theta_1-(a_2-b_2)sin\theta_1]^2}+\sqrt{b_2^2+(c_2-d_2)^2}+l_0 \tag{21}$$

The Jacobean matrix of the exosuit is:

$$\mathbf{J_v} = \begin{bmatrix} j_{11}^v & j_{12}^v \\ j_{21}^v & j_{22}^v \end{bmatrix}, \tag{22}$$

where:

$$j_{12}^v = \frac{[(a_1-b_1)(a_2-b_2-l_{ar})+d_1d_2]sin\theta_2+[d_1(a_2-b_2-l_{ar})-d_2(a_1-b_1)]cos\theta_2}{\sqrt{\begin{matrix}[d_1cos(\theta_1+\theta_2)+(a_1-b_1)sin(\theta_1+\theta_2)-d_2cos\theta_1-(a_2-b_2-l_{ar})sin\theta_1]^2+\\ [(a_1-b_1)cos(\theta_1+\theta_2)-d_1sin(\theta_1+\theta_2)-(a_2-b_2-l_{ar})cos\theta_1+d_2sin\theta_1]^2\end{matrix}}}$$

$$j_{11}^v = j_{21}^v = \frac{(a_3b_2-a_3a_2+b_3d_2)sin\theta_1-(b_3a_2-b_3b_2+a_3d_2)cos\theta_1}{\sqrt{[a_3+(a_2-b_2)cos\theta_1-d_2sin\theta_1]^2+[b_3-d_2cos\theta_1-(a_2-b_2)sin\theta_1]^2}}$$

$$j_{22}^v = 0$$

The detailed form of dynamic equation of the coupled system Eq. (12) is:

$$\begin{cases} M_{shoulder}^{cable} = \left[m_{ua}l_{cua}^2 + I_{ua} + m_{fa}\left(l_{ua}^2 + l_{cfa}^2 + 2l_{ua}l_{cfa}cos\theta_2\right) + I_{fa} + m_{load}\left(l_{ua}^2 + l_{cload}^2 + 2l_{ua}l_{cload}cos\theta_2\right)\right]\ddot{\theta}_1 \\ \quad +\left[m_{fa}\left(l_{cfa}^2 + l_{ua}l_{cfa}cos\theta_2\right) + I_{fa} + m_{load}\left(l_{cload}^2 + l_{ua}l_{cload}cos\theta_2\right)\right]\ddot{\theta}_2 - m_{fa}l_{ua}l_{cfa}sin\theta_2\left(2\dot{\theta}_1\dot{\theta}_2 + \dot{\theta}_2^2\right) \\ \quad -m_{load}l_{ua}l_{cload}sin\theta_2\left(2\dot{\theta}_1\dot{\theta}_2 + \dot{\theta}_2^2\right) + m_{ua}gl_{cua}sin\theta_1 + m_{fa}g\left[l_{ua}sin\theta_1 + l_{cfa}sin(\theta_1 + \theta_2)\right] \\ \quad +m_{load}g[l_{ua}sin\theta_1 + l_{cload}sin(\theta_1 + \theta_2)] \\ M_{elbow}^{cable} = \left[m_{ua}\left(l_{cfa}^2 + l_{ua}l_{cfa}cos\theta_2\right) + I_{fa}\right]\ddot{\theta}_1 + \left(m_{fa}l_{cfa}^2 + I_{fa} + m_{load}l_{cload}^2\right)\ddot{\theta}_2 \\ \quad +\left(m_{fa}l_{cfa} + m_{load}l_{cload}\right)l_{ua}sin\theta_2\dot{\theta}_1^2 + \left(m_{fa}l_{cfa} + m_{load}l_{cload}\right)gsin(\theta_1 + \theta_2) \end{cases} \tag{23}$$

References

1. Zhang, Y., Arakelian, V., Le Baron, J.: Design concepts and functional particularities of wearable walking assist devices and power-assist suits – a review. In: Proceedings of the 58th International Conference of Machine Design Departmants (ICDM 2017), pp. 436–441, Prague (2017)
2. Enoka, R., Duchateau, J.: Muscle fatigue: what, why and how it influences muscle function. J. Physiol. **586**(1), 11–23 (2008)
3. Jaworski, Ł., Karpiński, R., Dobrowolska, A.: Biomechanics of the upper limb. J. Technol. Exploit. Mech. Eng., **2**(1), 56–59 (2016)
4. Kazerooni, H.: Exoskeletons for human power augmentation. In: 2005 IEEE/RSJ International conference on intelligent Robots and Systems, pp. 3459–3464. IEEE, Edmonton (2005)
5. Marcheschi, S., Salsedo, F., Fontana, M., Bergamasco, M.: Body extender: Whole body exoskeleton for human power augmentation. In: 2011 IEEE international conference on robotics and automation, pp. 611–616. IEEE, Shanghai (2011)
6. Exhauss Homepage. http://exhauss.com/fr_produits.htm. Accessed 15 Apr 2021
7. Mao, Y., Agrawal, S.: Design of a cable-driven arm exoskeleton (CAREX) for neural rehabilitation. IEEE Trans. Rob. **28**(4), 922–931 (2012)
8. Jin, X., Aluru, V., Raghavan, P., Agrawal, S.K.: The effect of CAREX on muscle activation during a point-to-point reaching task. In: 2015 IEEE International Conference on Rehabilitation Robotics (ICORR), pp. 73–78. IEEE, Singapore (2015)
9. Lessard, S., et al.: Crux: A compliant robotic upper-extremity exosuit for lightweight, portable, multi-joint muscular augmentation. In: 2017 International Conference on Rehabilitation Robotics (ICORR), pp. 1633–1638, IEEE (2017)
10. Samper-Escudero, J.L., Giménez-Fernandez, A., Sánchez-Urán, M.Á., Ferre, M.: A cable-driven exosuit for upper limb flexion based on fibres compliance. IEEE Access **8**, 153297–153310 (2020)
11. Zhang, Y., Arakelian, V.: Design of a passive robotic exosuit for carrying heavy loads. In: 2018 IEEE-RAS 18th International Conference on Humanoid Robots (Humanoids), pp. 860–865. IEEE, Beijing (2018)
12. Zoss, A., Kazerooni, H., Chu, A.: On the mechanical design of the Berkeley Lower Extremity Exoskeleton (BLEEX). In: 2005 IEEE/RSJ International Conference on Intelligent Robots and Systems, pp. 3465–3472. IEEE, Edmonton (2005)
13. Drillis, R., Contini, R., Bluestein, M.: Body segment parameters. Artif. Limbs **8**(1), 44–66 (1964)